

Integrated Design Methodology for High-Precision/Speed Servomechanisms

Min-Seok Kim and Sung-Chong Chung

HYbrid Systems Design and Control LABORatory
School of Mechanical Engineering
Hanyang University, SungdongGu, Seoul 133-791, Korea

Abstract

An integrated design methodology is proposed to ensure the required high-speed and high-precision specifications in servomechanisms, where the interactions between mechanical and electrical subsystems will have to be considered simultaneously. Both the geometric errors referring to Abbe offset and the contour errors referring to circular motions are minimized through the design procedure satisfying allowable structural deformation errors, the relative stability and so on. The validity of the integrated design methodology is confirmed through design results.

Keywords: Abbe error, contouring error, high-precision/speed servomechanism, integrated design, nonlinear constrained optimization, stability

1. Introduction

High-precision/speed servomechanisms have been widely used in the manufacturing and semiconductor industries [1~2]. These specifications significantly exceed the axis motion capabilities of conventional ones. Therefore, it is necessary to devise special design concept to achieve this level of performance for high-precision/speed servomechanism.

In order to ensure the desired specifications in the servomechanism, an integrated design methodology is proposed [3~5], where the interactions between mechanical and electrical subsystems will have to be considered simultaneously during the design process.

In the first step of the integrated design process, it is necessary to focus on the strict modeling and analysis of those subsystems, individually. In addition to the modeling of subsystems, an accurate identification process of the mechanical subsystem is conducted. In the next step, the focus is on integrating subsystems to evaluate the desired performance of the servomechanism. For this purpose, we formulate the optimization problem that includes the relevant parameters of the servomechanism. Finally, simulations and numerical case studies are presented to demonstrate the effectiveness of the proposed design method.

2. Modeling of servomechanism

The mechanical characteristics of servomechanisms such as an equivalent inertia and stiffness have

significant effects on the design optimization.

The free-body diagram of servomechanism to look for dynamic behaviors is shown in Fig. 1. The mathematical model of the mechanical subsystem is constructed by developing the equation of dynamic motion between the motor and mechanical components of servomechanisms. The transfer function between a motor torque τ and rotational motor speed ω is described as Eq. (1).

$$G_p(s) = \frac{\omega(s)}{\tau(s)} = \frac{K_t}{J_m} \frac{s^2 + b_1}{s^3 + a_1 s^2 + a_2 s + a_3}$$

$$a_1 = \left(\frac{K_t K_{emf} + 1}{J_{eq}} \right), a_2 = \left(\frac{J_{eq} K_{eq} \eta + R^2 M_t K_{eq}}{J_{eq} M_t \eta} \right)$$

$$a_3 = \left(\frac{K_t K_{emf} + 1}{J_{eq}} \right) \frac{K_{eq}}{M_t}, b_1 = \left(R^2 + \frac{K_{eq}}{M_t} \right), R = \frac{p}{2\pi}$$
(1)

where, M_t is mass of table and workpiece, K_t is a torque constant, K_{emf} is a back-emf constant, η is the efficiency of driving mechanism, p is a ball-screw pitch, and K_{eq} , J_{eq} is an equivalent stiffness and inertia

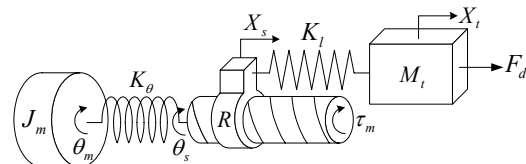


Fig. 1 Free-body diagram of mechanical subsystem.

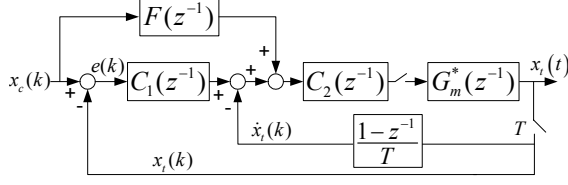


Fig. 2 Block diagram of electrical subsystem.

of mechanical subsystem, respectively.

A two-degree-of-freedom controller that consists of a PID feedback controller and a simple feedforward controller is considered in this paper. The task of the PID feedback controller is to eliminate the steady-state error and to reject the external disturbance such as friction forces. However, feedback controllers have several disadvantages such as poor tracking performance significant overshoots. To overcome these limitations, a direct velocity feedforward controller that adds a velocity command to the velocity feedback loop is considered.

The electrical subsystem structure can be presented as Fig. 2 and Eq. (2), where $F(z)$ is the feedforward controller, $C_1(z)$ is the P-controller as position control, and $C_2(z)$ is the PI-controller as velocity control.

$$F(z) = K_{ff} \left(\frac{z-1}{T_s z} \right), C_1(z) = K_{pp}, C_2(z) = K_{vp} \left(1 + \frac{K_{vi} z}{z-\alpha} \right) \quad (2)$$

From equation (1), (2) and Fig. 2, the open-loop transfer function $G_o(z)$ and closed-loop transfer function $G_c(z)$ of the servomechanism can be represented as

$$G_o(z) = \frac{C_2(z)G_m^*(z)[C_1(z)+F(z)]T_s z}{(1-F(z) \cdot C_2(z) \cdot G_m^*(z))T_s z + C_2(z)G_m^*(z)(z-1)} \quad (3)$$

$$G_c(z) = \frac{C_2(z)G_m^*(z)[C_1(z)+F(z)]T_s z}{(1+C_1(z) \cdot C_2(z) \cdot G_m^*(z))T_s z + C_2(z)G_m^*(z)(z-1)}$$

$$\text{where, } G_m^*(z) = (1-z^{-1})Z \left[\frac{G_m(s)}{s^2} \right]$$

3. Identification of servomechanism

An accurate identification process of the mechanical subsystem is conducted to verify the obtained mathematical model. The model structure for identification is the output error(OE) structure [6] which can be described as;

$$y(k) = \frac{B(z^{-1})}{F(z^{-1})}u(k) + e(k) \quad (4)$$

Parameters of the OE structure given in Eq.(4) are

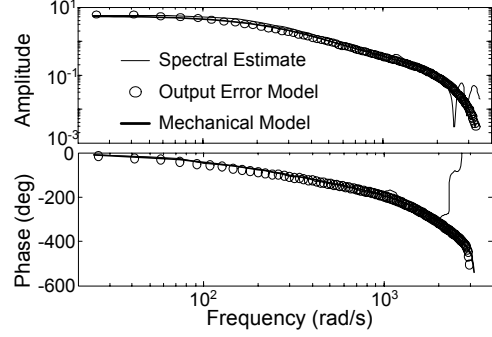


Fig. 3 Frequency response plot of identified system.

estimated using an least squares penalty function into a frequency domain description [6].

$$V(\theta) = \frac{1}{N} \sum_{k=1}^N \beta(k) [\omega(k) - \hat{\omega}(k, \varphi)]^2 \quad (5)$$

In general, an accurate mechanical subsystem model of servomechanisms is difficult to identify due to the nonlinear effects such as Coulomb friction, stiction and backlash. To avoid these effects that corrupt the identification, a biased-square wave input signal is used. The input signal which consists of a Gaussian pseudo-random binary sequence is used as the torque command for the closed current loop while the rotational motor speed is synchronously recorded.

We apply the identification process to a precision x-y positioning system. The positioning system basically consists of a ball-screw driving mechanism with AC-servo motors and amplifiers, an encoder, digital I/O interfaces, and a PC-based controller. A transfer function model is obtained for the input-output sequence using the MATLAB System Identification Toolbox [7].

For the single axis, a 3th-order model was obtained with coefficients $f = [1, -1.058, -0.08528, 0.2177]$, $b = [0.05741, 0.2937, 0.181]$. The magnitude and phase response of the mechanical subsystem model described in Eq.(1) are shown in Fig. 3 along with both the identified OE structure model and the power spectral estimates.

From these identification results, it can be confirmed that the mechanical subsystem model for an integrated design is reliably established.

4. Formulation of integrated design problem

In order to formulate an integrated design problem, the focus is on integrating subsystems to evaluate the desired performance of the servomechanism.

In circular motion, the system input for each axis is given as a sinusoidal wave and the amplitude of the

system output in steady state is the radius of actual circular motion. Therefore the contour error referring to the circular motion is represented as Eq.(6)

$$E_R = 1 - \frac{R_o}{R_i} = 1 - \sqrt{\operatorname{Re}\left[G_c\left(e^{j\omega_i T_i}\right)\right]^2 + \operatorname{Im}\left[G_c\left(e^{j\omega_i T_i}\right)\right]^2} \quad (6)$$

Geometric errors should be considered to design high-precision servomechanism. An angular error the worst type of geometric errors in servomechanisms is proportionally amplified by the distance between the central axis of the ball-screw and the table. This results in positioning errors called Abbe errors [8].

In order to guarantee the stability of the designed servomechanism, nominal and relative stability conditions which can be represented in terms of a gain and phase margin must be considered in the integrated design procedure.

A beam model on elastic foundation [9] is considered to obtain the structural deformation errors caused by the workpiece weight and cutting forces. In addition, the critical speed and buckling load of a ball-screw and saturation conditions of electrical sub-

system must be considered in the integrated design procedure. The list of constraints used in the integrated design procedure is shown in Table 1.

Using the modeling and performance analysis described above, we formulate a nonlinear constrained optimization problem including the relevant subsystem parameters of the servomechanism. Design variables \mathbf{x} , a multi-object function $F(\mathbf{x})$ and constrained conditions $g(\mathbf{x})$ are defined in this procedure. An Abbe offset, a ball-screw pitch and control parameters of the 2-D.O.F. controller are selected as design variables.

Consequently, the integrated design problem is formulated as the nonlinear constrained optimization problem given in Eq.(7).

Minimize

$$F(\mathbf{x}) = C_1 D_a + C_2 J_{eq} + C_3 E_R + C_4 \frac{1}{\omega_B}$$

subject to

$$g_i(\mathbf{x}) \leq 0, \quad i = 1, \dots, 8$$

$$\mathbf{x}_j^L \leq \mathbf{x}_j \leq \mathbf{x}_j^U, \quad j = 1, \dots, 7$$

$$\mathbf{x} = \{D_a, D_{bs}, p, K_{ff}, K_{pp}, K_{vp}, K_{vi}\}$$

(7)

Table 1 Constraints for integrated design.

| Description | Equation |
|---------------------|--|
| Maximum feedrate | $g_1: V_{\max} - V_{\max}^c < 0$ $V_{\max}^c = \lambda^2 \frac{D_{bs} P}{8\pi L_{sp}^2} \sqrt{\frac{E_{bs}}{\rho_{bs}}}$ |
| Maximum deformation | $g_2: \delta_c - \delta_c^* < 0$ $\delta_c = \frac{\beta}{2k} \left(\frac{2 + \cos \beta a_{tb} + \cosh \beta a_{tb}}{\sin \beta a_{tb} + \sinh \beta a_{tb}} \right) \cdot F_z$ |
| Buckling load | $g_3: F_c^x - P_b < 0$ $P_b = n \frac{\pi^2 E_{bs} I_{bs}}{L_{sp}^2}$ |
| Stability | <p>Nominal stability:</p> $g_4: z_i - 1 < 0$ $z_i = \{z: D_c(z) = 0\}, i = 1 \sim 7$ <p>Gain margin:</p> $g_5: A_m^* - A_m < 0$ $A_m = 1 / G_o(e^{j\omega_c T}) $ <p>Phase margin:</p> $g_6: \phi_m^* - \phi_m < 0$ $\phi_m = \angle [G_o(e^{j\omega_c T})] - \pi$ |
| Saturation | $g_7: \tau_c^{\max} - \tau_m^{\max} < 0$ $g_8: \tau_m^{\max} - T_{\max} < 0$ $\tau_m^{\max} = \frac{J_{eq}}{R} \frac{d^2}{dt^2} a_{\max}$ $\tau_c^{\max} = \max \left\{ \nu G_{sat}(e^{j\omega T}) \cdot X_c(e^{j\omega T}) \right\}$ |

where, $C_i (i=1 \sim 4)$ is the weighted factor of multi-object function.

5. Results of integrated design

Results of the integrated design (design variables and system performances) are listed in Table 2, 3. And the Bode diagrams and circular motion profiles of the designed servomechanism are shown in Fig. 4 and 5, respectively. The design results not only satisfy all the constraints but also improve the desired system performances.

From the Table 2 and 3, we can see that the Abbe offset and contour error is reduced by 37% and 90% of the initial design, respectively. In addition, it shows an

Table 2 Integrated design results: design variables.

| Design variable | Unit | Initial design | Integrated design |
|-----------------|-------|----------------|-------------------|
| $X_1(D_a)$ | m | 0.0410 | 0.0257 |
| $X_2(D_{bs})$ | m | 0.016 | 0.0125 |
| $X_3(l)$ | m | 0.005 | 0.0132 |
| $X_4(K_{ff})$ | V/V | 0.1 | 0.1400 |
| $X_5(K_{pp})$ | V/V | 100 | 98.6717 |
| $X_6(K_{vp})$ | V/V | 1 | 2.9772 |
| $X_7(K_{vi})$ | V/V | 0.1 | 0.3974 |

Table 3 Integrated design results: system performance.

| Performance index | Unit | Initial design | Integrated design |
|-------------------|----------------|-----------------------|-----------------------|
| E_R | % | 6.6800 | 0.0668 |
| f_B | rad/s | 12.717 | 40.030 |
| J_{eq} | $kg \cdot m^2$ | 1.03×10^{-4} | 8.13×10^{-5} |
| τ_{max}^c | $N \cdot m$ | 1.29 | 0.829 |
| A_m | dB | 86.828 | 25.201 |
| ϕ_m | degree | 81.749 | 75.761 |

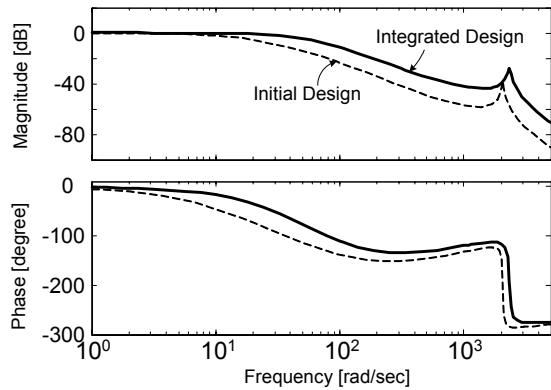


Fig. 4 Bode diagram of integrated designed system.

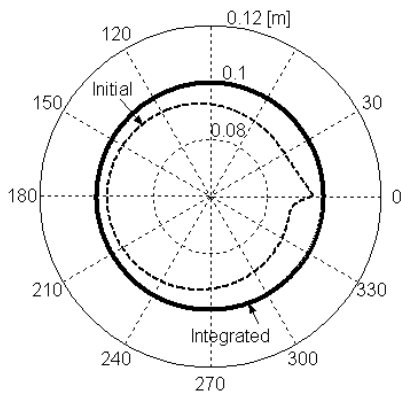


Fig. 5 Circular motion profile for integrated design.

increase of three times over the initial design of a system bandwidth. Therefore a high precision/speed servomechanism has been designed by the proposed design methodology.

The decrease of the relative stability shown in Table 3 means the low-gain of initial electrical subsystems and over design of initial mechanical subsystems.

From these results we can confirm the effectiveness of the integrated design methodology

6. Conclusion

An integrated design methodology is proposed to design a high speed/precision servomechanism. In addition to the strict modeling of subsystems, an accurate identification process of the mechanical subsystem is conducted. Both the geometric error and the contour error are minimized through the integrated design procedure. The validity of the integrated design methodology is confirmed through design results.

Analysis of the simulation results from the integrated design methodology allows better understanding of the dynamic behavior and interactions of the servomechanism. Furthermore, the proposed design methodology offers not only the improved possibility to evaluate and optimize the dynamic motion performance of the servomechanism, but also improves the quality of the design process to achieve the required performance for high-precision/speed servomechanisms.

References

- Schulz, H. and Moriwaki, T., 1992, "High-Speed Machining", *Annals of the CIRP*, Vol. 41, No. 2, pp. 637~643.
- Tlusty, J., 1993, "High-Speed Machining", *Annals of the CIRP*, Vol. 42, No. 2, pp. 733~738.
- Isermann, R., 1996, "On the Design and Control of Mechatronic Systems-A Survey", *IEEE Trans. On Industrial Electronics*, Vol. 43, No. 1, pp. 4~15.
- Skelton, R. E., 1997, "Integrated Design, Modeling and Control of Structure", *Proc. of KACC*, pp. 1~4.
- Chang, H. D. and Chung, S. C., 2002, "Integrated Design of Radial Active Magnetic Bearing Systems Using Genetic Algorithms", *mechatronics*, Vol. 12, pp.19~36.
- Ljung, L., 1999, *System Identification-Theory for the User*, Prentice Hall PTR, New Jersey, pp.79~246
- MATLAB System Identification Toolbox User Guide*, Mathworks, Inc., 2000.
- Nakazawa H, 1994, *Principles of Precision Engineering*, Oxford University Press, N. Y.
- Ugral, A. C. and Fenster, S. K., 1987, *Advanced Strength and Applied Elasticity*, Elsevier, New York, pp. 300~315.